ISBN: 978-3-95450-219-6 ISSN: 2226-0366 doi: 10.18429/JACoW-LINAC2024-TUPB067

RF AND MULTIPACTING ANALYSIS OF THE HIGH-POWER COUPLERS OF IFMIF/EVEDA RFQ AND ESS DTL

F. Grespan, C. Baltador, L. Bellan, M. Campostrini, M. Comunian, E. Fagotti, L. Ferrari, A. Palmieri, A. Pisent, C. Roncolato, INFN- LNL, Legnaro, Italy
D. Nicosia, L. Page, R. Zeng, ESS, Lund, Sweden
L. Y. Gong, IMP, Chinese Academy of Sciences, Lanzhou, China
F. Cismondi, F. Scantaburlo, IFMIF/EVEDA Project Team, Rokkasho, Japan
A. De Franco, QST, Rokkasho, Japan
H. Kobayashi, KEK, Tsukuba, Japan

Abstract

The performances and failure cases of the power couplers of the IFMIF/EVEDA RFQ and ESS DTLs have been analysed with dedicated high-power test campaigns and Multi-Pacting (MP) simulation methods. The paper presents test and simulation methodology, results, and inputs for the next activities.

INTRODUCTION

IFMIF/EVEDA RFQ power couplers

Eight tetrode RF amplifiers at 175 MHz - numbered 1A…4A, 1B … 4B - feed the IFMIF/EVEDA RFQ [1] for 1.6 MW total power capability. The net power need is $P_{TOT}[1.3MW] = P_{cav}[650kW] + P_{beam}[650kW]$. Beam performances in pulsed mode have been demonstrated in 2019 [2]. In RF conditioning beam loading is absent, so each coupler operates with $P_{REV} \approx 13\%$. The couplers (Fig. 1) are coaxial magnetically coupled loops, without bias. A coaxial planar alumina window separates vacuum from air, vacuum sealing being provided by Viton O-rings. The impedance matching between window and line is given by reducing the inner conductor radius. RF windows are coated with 1.5 -3 nm TiN layer. The alumina is not directly water cooled. The couplers have been designed and tested on a test cavity at full power (200 kW-CW) at INFN-LNL in 2015 [3].

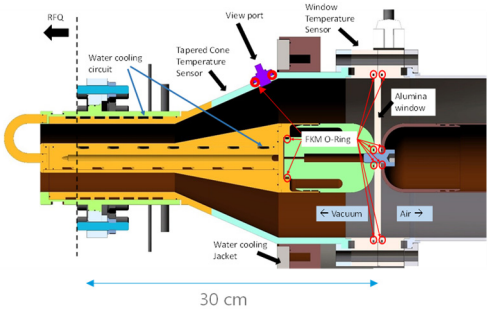

Figure 1: Sketch of the IFMIF coupler. The diagnostics and the positions of Viton O-ring are shown.

During RFQ RF conditioning operations toward CW [4] (2019-2023), 5 of the 8 couplers showed anomalous temperature increases of the external conductors. Two improvements of cooling capability have been implemented: in 2019 water jackets were applied on the external conductor. In 2023 the inner conductor cooling was improved, after finding O-rings melted, once reached 60% average power. In the same inspection the alumina was found coloured, as well as the copper inner conductor (Fig. 2). Nonetheless, in November 2023, after reaching 25% average power, a vacuum leak occurred again.

An experimental and theoretical analysis of the electron activity in the couplers was carried out to clarify the power heat source capable to heat the O-ring at melting temperature (180°C).

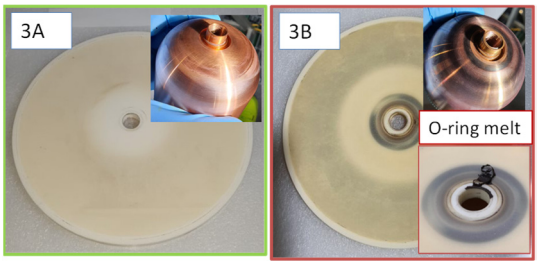

Figure 2: Status of "cold" (left) and "hot" (right) coupler.

ESS DTL's Power Couplers

One 2.9 MW klystron at 4% duty cycle feeds each of the 5 DTLs (352 MHz). The net power need is $P_{TOT}[2.2MW] = P_{cav}[1.1MW] + P_{beam}[1.1MW]$, coupled to the cavity by 2 iris couplers placed on the bottom of the DTLs. The air-vacuum separation between cavity and wave guide is provided by a pillbox-type alumina RF window, water cooled and coated with 2 nm TiN layer. Windows are connected to the coupler box with a WR2300 HH flange (Fig. 3). The windows have 2 view ports (air and vacuum sides). The sealing between the RF window and coupler box is an EPDM gasket, without RF joint protections. The RF windows were tested to full power in 2020.

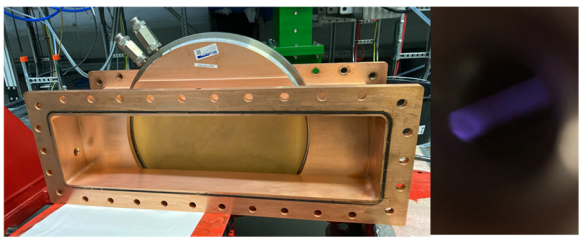

Figure 3: One of the ESS DTL RF windows. Brown coloration melted O-ring and light is shown.

In 2023 DTL1-2-3-4 started high power RF operation at ESS Lund, reaching full performances [5]. But, after 6 weeks of operations, light started on both vacuum and air

ISBN: 978-3-95450-219-6 ISSN: 2226-0366 doi: 10.18429/JACoW-LINAC2024-TUPB067

sides of DTL2 and DTL3 RF windows, without evidence of either excessive P_{REV} or overheating. DTL1 and DTL4 are ok. After an inspection in July 2023, O-rings were found melted (for RF leak) and the windows show a yellow-brown colour on the area exposed to RF, while the RF hidden surfaces are maintained whiter (Fig. 3).

Then we moved to design a new metallic gasket and to RF test the windows offline. Also, a theoretical analysis of MP has been done in parallel of the IFMIF case.

MP ANALYSIS METHODOLOGY

CST simulations of MP are performed using SEY of alumina and copper from Refs. [6, 7]. The initial electron distribution follows studies performed in [8, 9]. MP evolution is studied as first without space charge (S.C.) saturation. The S.C. effect is included to evaluate the entity of power deposition by electron activity (see IFMIF RFQ case) or the severity of MP for those geometries where it is hard to eliminate MP phenomena (see ESS DTL case). The simulation method, common for IFMIF and ESS, is:

1. Large section of the window/coupler implemented into the CST simulation.
2. Volume of interest filled with 10000-20000 starting electrons, in the energy range [0.0001-10] eV, to reveal the possible criticalities of the geometry.
3. Electron tracking, with/without S.C., is then included for different RF power levels.
4. Thermal simulations, based on electron's power deposition.
5. Comparison with the coupler's experimental results and damages.

The results have been validated by recognizing the coloured surfaces observed on the alumina and metal components of the windows, and with the correspondence with high temperatures and vacuum reactions at different power.

IFMIF/EVEDA RFQ COUPERS

RF Measurements and Observations

For a better understanding of the MP on the IFMIF-EVEDA RFQ couplers, RF measurements were performed injecting RF power into the RFQ under various reflection conditions and recording the analogic light intensity signal. The equivalent power deposited in a transmission line at the position z from the origin is given by:

$$P_{eq}(z,f,f_0) = \frac{|V_{eq}(z,f,f_0)|^2}{2Z_0} = \frac{|V_{FWD} + V_{REV}(z,f,f_0)|^2}{2Z_0}$$

Z_0 being the characteristic impedance of the line. The origin is the coupler port and z are negative moving towards the power source. The reflection coefficient $\Gamma(z,f,f_0)$ is changed by thermally detuning the cavity frequency f_0 and keeping the drive frequency f constant at 175 MHz.

Figure 4 shows the comparison between measured values of P_{REV} at the couplers 1A ("hot") and 4B ("cold") in different detuning conditions: P_{REV} of coupler 1A presents a deformation with respect to theoretical curve. Figure 4 also reports the light intensity (approx. -25 mV/1 lux) detected at the viewport of coupler 2A. Figure 5 represents the light intensity as a function of the P_{eq} evaluated at the window location (≈30 cm backwards from the coupler port), showing a good linear correlation. Moreover, since coupler temperatures increase even at low DC% proportionally to the light signal, we conclude that a significant plasma is established on that volume by MP: residual gas ionized by electrons emits light and it also perturbs the reflected power, showing a -5 kHz frequency shift in the 1A chain. The 5 hot power couplers present light activity at all P_{FWD} > 40 kW and at all tested duty cycles.

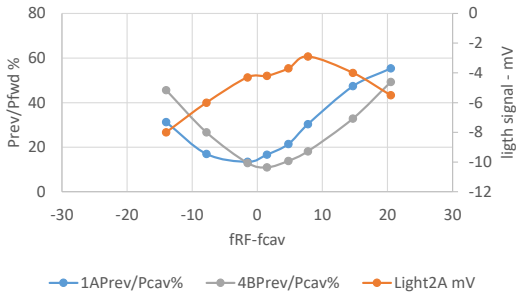

Figure 4: Measured P_{REV} @ couplers 1A ("hot") and 4B ("cold") and light @ coupler 2A ("hot") vs. detuning.

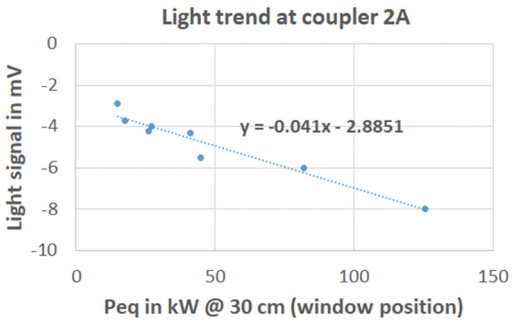

Figure 5: Light intensity as a function of P_{eq} (coupler 2A).

MP Analysis of IFMIF/EVEDA RFQ Couplers

For simulations the coupler is divided in 3 sections to identify geometries affected by MP: RF window section, the taper-cone and the final coaxial section. The final coaxial section and the second part of the taper-cone do not show MP. Therefore, we focused on the RF window section, the most delicate for the presence of alumina and O-rings. Figure 6 shows the correspondence between simulated electron flows and visual inspection of one damaged coupler. Simulations show that MP is triggered by the coaxial inner and outer dimensions and the large radius curvature of the anchor. This large radius focuses the electrons

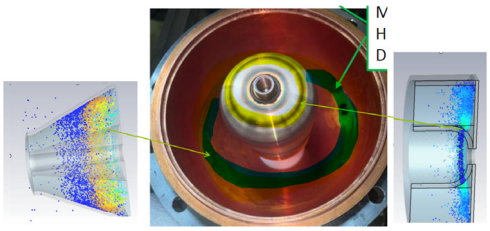

Figure 6: MP simulations and photo of the anchor zone of one of the "hot" couplers. Marks of MP are pointed out.

ISBN: 978-3-95450-219-6 ISSN: 2226-0366 doi: 10.18429/JACoW-LINAC2024-TUPB067

when the field is inward directed, potentially generating large surface power depositions. To evaluate the temperature at the O-ring, a simulation with S.C. saturation has been done at P_{FWD} = 80 kW, with P_{REV}=13%. In the steady state (MP saturated), we calculated power deposition onto inner conductor by electron collisions. The electrons generate a power density of 50 W/cm^2 in that zone. COMSOL thermal simulations show that the temperature close to the O-ring can reach 250°C (Fig. 7), which can explain the damages.

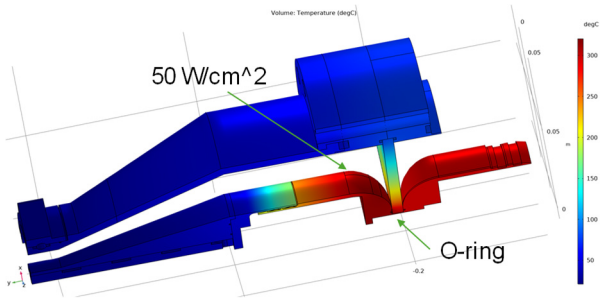

Figure 7: COMSOL thermal simulation, with a power density of 50 W/cm^2 calculated from MP.

ESS DTL RF WINDOWS

Offline RF Power Test

Nine of the 13 RF windows procured for the ESS DTLs are under test in an offline test bench, using the DTL5 klystron. DTL1 and DTL4 windows have been kept on the cavities. The waveguide vacuum box was updated with a larger pumping port and a new aluminium gasket was designed to replace O-rings both on the test box and on the DTL installation. These improvements have been crucial to start with vacuum < 1.0 e-7 mbar. Besides the hardware, we improved the conditioning routine [10]. Without going into the details of the conditioning procedure, we just report that a part the protection interlocks (vacuum, arcs, temperatures), the PFWD ramps are driven by soft thresholds, i.e., PFWD can increase only if vacuum <2.5e-7 mbar AND if the light signal (on top of the noise) < 25 mV (Fig. 8). Test is considered successful if vacuum < 1.0e-7 mbar at full power and light is conditioned out after 12 hrs endurance test in TW at full power. Test is done also in standing wave.

The summary of the tests is that 3 of the 5 arcing windows are confirmed lightening. We are trying to refurbish one window with the producer. 2 arcing windows has been "re-processed" by RF and MP is now conditioned away. 4 windows, never installed on the DTLs before, passed the test. All the windows have very strong MP levels at PFWD < 400 kW (Fig. 8).

MP Analysis of the ESS DTL RF Windows

We analysed the sensitivity to MP of ESS DTL windows as described in the previous paragraph. These windows are prone to MP due to similar characteristics of the IFMIF RFQ couplers: gap dimension and large curvature of the surface in front of the alumina. Figure 9 visually shows the similarity of the simulated MP electrons with the grayish on the alumina disk, cut-out for refurbishment. The reaction to MP at PFWD < 400 kW observed in conditioning (Fig. 8) is confirmed by simulations (Fig. 10).

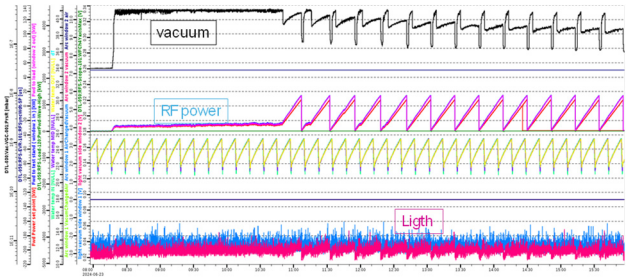

Figure 8: RF Conditioning plot of one pair of DTL window. N.B. vacuum soft threshold limiting PFWD ramp and the strong vacuum reaction to MP below 400 kW.

Based on these results, we studied a new geometry with improved performances, changing the pillbox gap distances and reducing the round edge curvature. The comparison between original and new geometry is shown in Fig. 10: the geometry optimization reduces the electron multiplication of a factor 5 (black curves) with respect to the original design (orange curves).

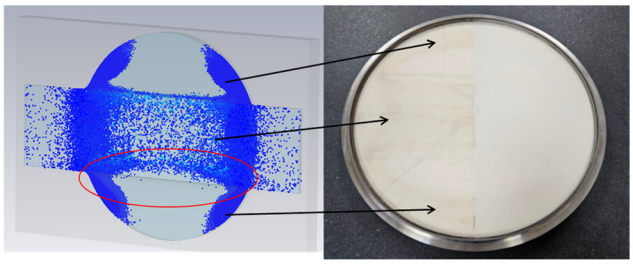

Figure 9: MP simulations and photo of one of the alumina. Shadows of MP are pointed out.

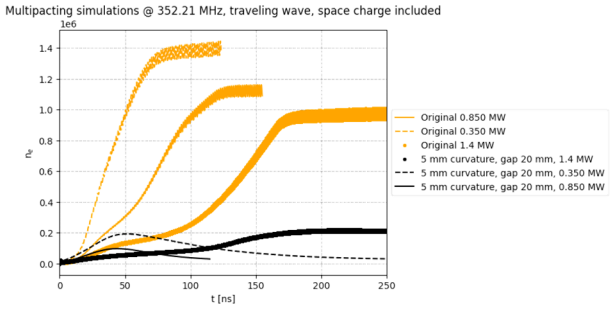

Figure 10: ESS DTL window original/new design, here compared as for MP e$^-$ multiplication at S.C. saturation.

CONCLUSIONS AND PERSPECTIVES

To summarize the reported analysis: first, RF operation in good vacuum (< 1.0e-7 mbar) is the crucial ingredient of RF window performances and lifetime: MP electrons are usually conditionable with time, while the ionized residual gas can contaminate the coated alumina surface causing SEY deterioration. TiN coating layers should be sufficiently thick to guarantee good uniformity and coverage of the alumina. RF design can be checked for MP, since often there is room for optimization.

ISBN: 978-3-95450-219-6 ISSN: 2226-0366 doi: 10.18429/JACoW-LINAC2024-TUPB067

REFERENCES

[1] K. Hasegawa *et al.*, "LIPAc (linear IFMIF prototype accelerator) beam commissioning & future plans", in *Proc. IPAC'23*, Venice, Italy, May 2023, pp. 15-20. . doi:10.18429/JACoW-IPAC2023-MOYD2

[2] F. Grespan *et al.*, "IFMIF/EVEDA RFQ beam commissioning at nominal 125 mA deuteron beam in pulsed mode", in *Proc. IPAC'20*, Caen, France, May 2020, pp. 21-25. doi:10.18429/JACoW-IPAC2020-TUVIR11

[3] E. Fagotti *et al.*, "The couplers for the IFMIF-EVEDA RFQ high power test stand at LNL: design, construction and operation", in *Proc. LINAC'14*, Geneva, Switzerland, Aug.-Sep. 2014, paper TUPP093, pp. 643-645.

[4] A. De Franco *et al.*, "RF conditioning towards continuous wave of the RFQ of the Linear IFMIF Prototype Accelerator", *J. Phys.: Conf. Ser.,* vol. 2687, p. 052019, 2024. doi:10.1088/1742-6596/2687/5/052019

[5] F. Grespan *et al.*, "Status and overview of the activities on ESS DTLs", in *Proc. IPAC'23*, Venice, Italy, May 2023, pp.851-854. doi:10.18429/JACoW-IPAC2023-MOPL127

[6] I. Bojko, N. Hilleret, and C. Scheuerlein, "The Influence of air exposures and thermal treatments on the secondary electron yield of copper", *J. Vac. Sci. Technol. A*, vol. 18, pp. 972-979, 2000. doi:10.1116/1.582286

[7] J. Lokiewicz *et al.*, "Characteristics of TiN anti-multipactor layers reached by Titanium vapor deposition on alumina coupler windows", in *Proc. 11th Workshop on RF Superconductivity (SRF'03)*, Lubeck/Travemünder, Germany, Sep. 2003, paper THP31, pp. 697-699.

[8] G. Toby *et al.*, "Multipacting analysis of warm linac RF vacuum Windows", in *Proc. IPAC'21*, Campinas, SP, Brazil, May 2021, pp. 1044-1047. doi:10.18429/JACoW-IPAC2021-MOPAB336,

[9] S. V. Langellotti, N. M. Jordan, Y. Y. Lau, and R. M. Gilgenbach, "CST particle studio simulations of coaxial multipactor and comparison with experiments", *IEEE Trans. Plasma Sci.*, vol. 48, no. 6, pp. 1942-1949, Jun. 2020. doi:10.1109/TPS.2020.2981257

[10] C. Arcambal *et al.*, "Conditioning of the first mass production power couplers for the ESS elliptical cavities", in *Proc. 19th Int. Conf. RF Superconductivity (SRF'19)*, Dresden, Germany, Jun.-Jul. 2019, pp. 288-292. doi:10.18429/JACoW-SRF2019-MOP086